Overlapped pulsed pumping of tandem pumped fiber amplifiers to increase achievable pulse energy

Andrew Malinowski, Jonathan H. V. Price and Michalis N. Zervas, *Member, IEEE*

***Abstract*—It has been reported previously that in the regime appropriate for amplifying femtosecond pulses using the chirped pulse amplification technique in Yb-fiber sources that sub-micro-second pulsed tandem pumping not only provides the thermal benefits of c.w. tandem pumping but also enables strong suppression of ASE. In that case, the pump pulse preceded the signal pulse train. Here we propose a tandem pumping scheme in rare-earth-doped fiber amplifiers, where a train of signal pulses is amplified by a pump pulse which is almost exactly temporally overlapped. Simulations demonstrate that this can be used to create uniform gain across the signal pulse train, even at very high total pulse energies where there would be significant gain shaping in the previous case. In addition the pump is absorbed in a much shorter length, which increases the threshold for nonlinear effects and gain of greater than 26 dB is shown to be readily achievable in an amplifier as short as 1.5 m. This results in increased extractable energy before reaching the threshold for limiting nonlinear effects such as stimulated Raman scattering. These attributes should be attractive for high energy, high average power, ultrashort pulse, coherently combined fiber laser systems.**

***Index Terms*— Pulsed fiber amplifier, tandem pumping**

I. Introduction

FIBER lasers are excellent high average power sources due to their high efficiency, stable long-term performance, their waveguiding character and their nearly ideal geometry for heat dissipation [1]. Driven by manufacturing applications, powers of 100 kW have been demonstrated by incoherently combining c.w. fiber lasers. At this 100 kW power level, even fiber lasers require careful thermal management and technical issues arise such as reliably splicing the large numbers of pump diodes. Tandem-pumping, where one or more fiber lasers pump a fiber amplifier, addresses both issues [2-4]. It enables the majority of the brightness enhancement to be performed in the pump fiber amplifier and distributes quantum defect heating across the pump and signal fiber amplifiers. Hence, the most powerful fiber lasers realized to date are tandem-pumped systems [5, 6].

Ultrashort, ps and fs pulse lasers with peak intensity sufficient for plasma generation can offer a route for precision marking and ablation in the industrial setting and power scaling of such sources would enable higher throughput. There are also very ambitious plans for using fiber lasers for future electron accelerators [7] and for space debris management [8]. Such applications will require ultrashort pulses with tens of Joules of energy, which, for fs pulses, is currently only achievable with Ti:Sapphire lasers. However, they also require repetition rate scaling from the current 1 Hz level to tens of kHz so Ti:Sapphire lasers are unsuitable and the efficiency and the average power scaling ability of fiber lasers become attractive. To date, very large mode rod-type fibers have been used to achieve >1 mJ output at >100 W average power levels using the same directly diode-pumped double-clad fiber geometry as used in c.w. lasers. However further mode-size and hence energy scaling is challenging in single core fibers and average power scaling is limited by the onset of transverse modal instabilities [9, 10]. To address this challenge, the concept of using a coherently combined Yb-fiber amplifier array has been developed and test-bed femtosecond systems currently envisioned for accelerators would produce 40 J pulses at a repetition rate of 10 kHz and an average power of 40 kW. However, the complexity of coherently combining the output in a stable way and the high average power will create tight tolerances on the thermal fluctuations permissible in the multiple fiber amplifiers, and on levels of amplified spontaneous emission (ASE), which is typically a significant fraction of the output in low pulse-repetition-rate fiber lasers.

In pulsed fiber lasers the high peak powers and tightly confined wave-guide mode can result in unacceptable levels of self-phase-modulation (SPM) and stimulated Raman scattering (SRS). One reason that the practical use of tandem pumping for power scaling has so-far been largely confined to high power c.w. systems based on Yb-fiber amplifiers has been that

This paragraph of the first footnote will contain the date on which you submitted your paper for review.

J. H. V. Price was supported by funding from EPSRC (UK) Centre for Innovative Manufacturing in Photonics: EP/H02607X/1. This work was supported in part by the EPSRC (UK) EP/M014029/1 and the AFOSR grant FA9550-14-1-0382. This project was supported by the Royal Academy of Engineering under the Research Chairs and Senior Research Fellowships scheme. The first two authors contributed equally to this paper. The data for this paper can be found at: http://dx.doi.org/10.5258/SOTON/399217

A. Malinowski is with SPI Lasers, Southampton SO30 2QU, U.K. (e-mail: andy.malinowski@spilasers.com).

J. H. V. Price is with the Optoelectronics Research Centre, University of Southampton, Southampton SO17 1BJ, U.K. (e-mail: jhvp@orc.soton.ac.uk).

M. N. Zervas is with the Optoelectronics Research Centre, University of Southampton, SO17 1BJ, U.K., and holds an RAEng Research Chair in Advanced Laser Technologies for Future Manufacturing (e-mail: m.n.zervas@soton.ac.uk).

the in-band absorption cross-sections in the 1010-1030 nm range are lower than at the 975 nm absorption peak and so efficient pump-absorption requires that the device length is increased, leading to limiting nonlinear effects. However, it has been demonstrated that converting the output of low-brightness multimode diodes using a fiber laser to create a single mode pump source would enable core-pumping of the final tandem pumped amplifier and then increased pump absorption enables device lengths of ~2-3 m [11]. Pulsed operation typically produces higher ASE than in c.w. amplifiers, because higher maximum inversion is reached for the same average power. Then ASE can even be the limiting factor on maximum extractable pulse energy.

In our previous paper we described how the use of a pulsed pump for tandem pumping suppresses ASE by up to 20 dB by reducing the time over which the Yb ions are highly inverted [11]. In that paper both the pump laser and the signal amplifier fiber were used for energy storage. The pump laser converted the c.w. multimode diode output to short pulse single-mode format and the signal fiber received and stored all the pump pulse energy before it was then extracted by the output pulse. However, this approach did not mitigate the very definite limit to the pulse energy which can be extracted. This is due to the limited amount of energy which can be stored in a fiber prior to extraction by the signal pulse. When the entire fiber has reached the saturated inversion level for the pump wavelength, no more energy storage is possible. In practice, well before this level has been reached, ASE emission reaches an unacceptable level. In this paper, we show that a temporally overlapped pulsed pumping scheme allows us to circumvent this pulse energy limit by achieving much faster energy transfer from the pump pulse to signal pulse, and it also achieve even lower ASE, as well as seeing improvements which will suppress nonlinear effects. We used the same signal-fiber parameters as previously because they relate to widely used large-mode-area few-moded fiber designs and because this enables direct comparison of achievable energies with the previous results. (The pump and signal wavelengths are the same as in our previous paper to enable such comparison [11].)

To minimize the number of coherently combined fibers in power scaling applications, pulse-train formats that increase the energy per channel will be necessary. There are several techniques, such as burst mode [12-15] or divided pulse amplification (DPA) [16, 17] that require amplification of a pulse train having a duration of several tens or hundreds of nanoseconds. The first study of Yb-fiber sources that sub-micro-second pulsed tandem pumping considered a signal pulse burst with duration of 70 ns. In that case a relatively long, 500 ns, pump was used to invert the gain medium before the arrival of the signal pulse which then extracted the stored energy and because the pump pulse was both substantially longer than the signal pulse and finished before the start of the signal pulse, the extractable energy was clamped by the saturation energy of the fiber or nonlinear effects at the leading edge of the pulse (which experienced highest gain). The possibility also exists to overlap the pump and signal pulses in time. This provides additional benefits because pulse energy limitations due to the saturation energy of the amplifier and due to nonlinear effects are significantly improved. Here we show that this pulse energy can be significantly increased to levels above the saturation fluence if the pump and signal pulse are temporally overlapped. The nonlinear limitations are also reduced because the pump is absorbed in a shorter length and the gain is equalized from the leading edge to the trailing edge of the pulse-burst. The systematic simulations presented below show a path to implementing these suggested approaches in a practical system.

The structure of the paper is as follows: Section II details the parameters and numerical techniques applied in the simulations; Section III shows the simulation results; Section IV describes how the results impact on thresholds imposed by nonlinear interactions in the amplifier; Section V shows possible pumping schemes; Section VI provides a discussion of the benefits of the scheme and Section VII lists the conclusions.

II. Description of the Numerical Model

We model a Yb^{3+} fiber amplifier and simulate tandem pumping using a rate equation model [18, 19] which considers signal gain in the amplifier, broadband ASE, background loss and Rayleigh backscattering. An effective mode overlap with the dopant is calculated based on the index and doping profiles of the fiber. The quasi-three-level Yb^{3+} system is assumed to have two energy manifolds [20], so the model deals with the interaction between a number of signals and a single inverted population. The pump and signal are treated as spectrally narrow. This is a reasonable approximation for nano- or picoseconds pulses. The ASE is described by a number of channels with frequency bandwidth equal to the frequency spacing between the channels, seeded with the standard photon-per-mode per polarization state assumption. Forward and backward propagating channels are modeled but the only direct interaction between the forward and backward propagating waves is the Rayleigh back-scattering term. The rate equations were solved numerically using the method of characteristics [18], with a spatial grid of 2.5 cm, and a time step corresponding to the signals travelling one spatial step. The evolution of the cavity is modeled over several cycles of pumping, until the results over each cycle converge. This generates information on the start-up dynamics of the amplifier, but only the performance after the amplifier has stabilized will be discussed in this paper. Nonlinear effects are not included in the simulations, but methods for avoiding nonlinear limitations will be discussed in Section IV.

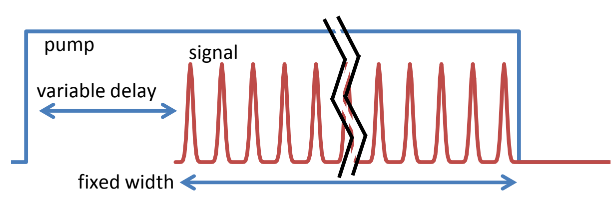

Fig. 1 Schematic of input pump and signal pulses

Our simulations used 92 ASE channels, equally spaced in frequency and covering the range 1000-1150nm. Increasing the number of channels or the wavelength range covered did not significantly affect the results obtained. Absorption and emission cross-sections were taken from Ref. [21].

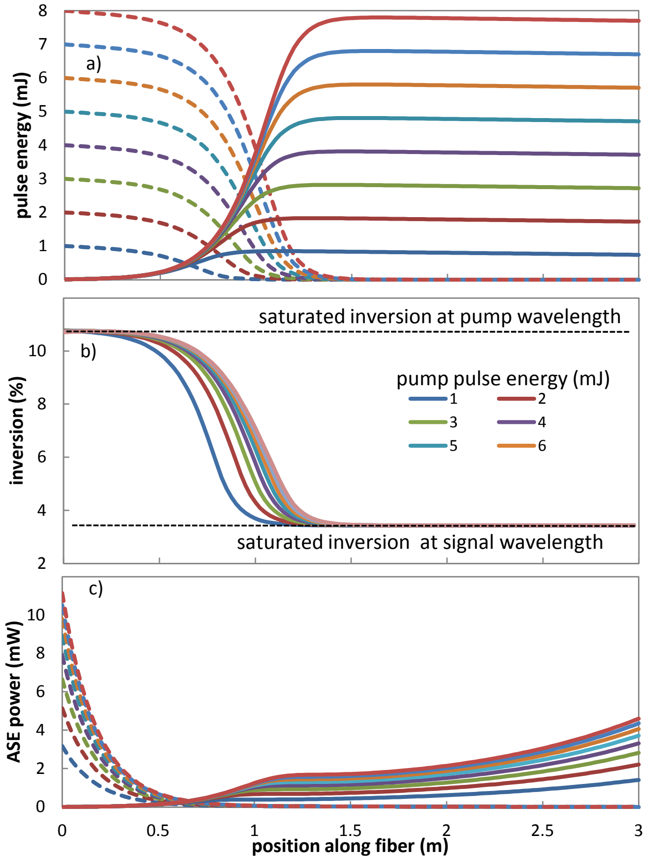

Fig. 2 (color online) a) evolution of the overlapped pump (dashed) and signal (solid) pulses along the amplifier fiber, b) inversion(N_2/N), c) forward (solid) and backward (dashed) time-averaged ASE powers along the fiber, for different pump pulse energies. In b) saturated inversion refers to the inversion level at which absorption becomes zero for the specified wavelength

Pump and signal are both launched into the core of the fiber and are co-propagating in the LP_{01} mode. In this paper we focus on the case of a sequence of nominally identical signal pulses with close spacing (as in divided pulse or burst mode operation). A schematic of the pulses is shown in Fig. 1. The pump pulse has a wavelength of 1018 nm and an adjustable duration. The input signal consists of a string of shorter pulses at wavelength 1045 nm with a fixed total duration. For the simulations presented here, the individual signal pulses were modeled as having Gaussian temporal envelope, with width 2 ns and spacing 8 ns and because the peak power is limited by nonlinear effects to ~100 kW. A burst mode format has been adopted using a train of 32 pulses (total duration 250 ns). The parameters were chosen to avoid excessive nonlinear effects. (Details shown in Section IV.) The pump was modeled as a flat-top rectangular pulse. It was found that the shape of the individual signal pulses had minimal effect on the output powers obtained. The pump pulse overlaps the string of signal pulses. The duration and relative delay of the pump pulse can be varied to produce optimised amplification. The optimum pump pulse was typically a few tens of ns longer than the signal pulse train, i.e. of order 300 ns.

As in ref. [11], we simulated a 14 μm core fiber (effective area (A_{eff}) of 130 μm^2) with a single transverse mode (LP_{01}) and Ytterbium doping concentration of $4.4\times10^{26}/m^3$. A value for background loss typical of a commercial fiber was chosen (10 dB/km) and the strength of the back-scattering (4×10^{-3} dB/km) was based on our measured values for fibers of similar composition. The value is about an order of magnitude larger than calculated from for the Rayleigh backscattering in a silica fiber of NA 0.1 [22], but known sources of distributed scattering in active fibers [23] account for the difference. In fact, backscattering was found to have a negligible effect on the results of the simulations.

III. Results

Simulations were first carried out to investigate the gain dynamics of the amplifier and to determine an optimum Yb-fiber length. In these simulations the pump pulse started 4 ns before the peak of the first signal pulse and continued until the end of the last signal pulse. In all simulations the total energy of the input signal pulse train was 0.01 mJ and the pulse repetition rate was set at 10 kHz.

Figure 2 shows the evolution of the pulses in a 3 m length of fiber for various pump pulse energies. The pump and signal are co-propagating. In Figs. 2a) and c) pump and signal are represented by dashed and solid lines respectively. It can be seen that transfer of power from the pump to the signal is complete after ~1.5 m. After this 1.5 m length the main processes are reabsorption of the signal and ASE build-up, as shown by the inversion level in Fig. 2(b) and the forward ASE average power in Fig. 2(c). ASE is a slow process and the signal power drops by <2% from its maximum value after 3 m propagation.

The imulations with up to 8 mJ overlapped pulses show no significant fall-off of conversion efficiency, and ASE levels remained low. This is because the energy for each individual pulse in the train is provided by the pump in the time between subsequent pulses. Output will only be clamped when the energy of an individual pulse is comparable to the amount of energy storable in the fiber. In practice, other limits will come into play well before this (see section IV).

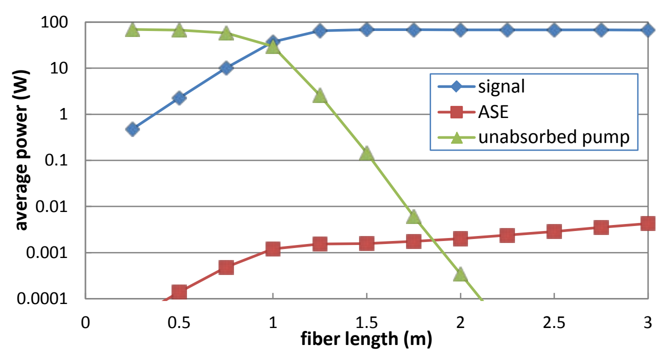

Fig. 3 The average powers of the amplified signal, ASE and unabsorbed pump at the output of the amplifier fiber as a function of amplifier length for a

pump power of 70 W (7 mJ overlapped pump pulses).

Simulations were carried out with fixed 7 mJ pump pulse energy for a range of fiber lengths. We focus on this particular pulse energy because we estimate that it is the highest energy where the peak power of the pulses remain below the threshold for nonlinear effects (see section IV for details). Figure 3 shows the dependence of output signal power, output ASE power and unabsorbed pump power on the length of the fiber. As suggested by the gain dynamics in the 3 m fiber, the optimum length to achieve both maximum signal power and the lowest ratio of ASE to signal power is ~1.5 m. At this length the pump absorption is 99.8%. At this fiber length, the signal conversion efficiency with respect to absorbed pump is 97.4%. The balance is indistinguishable from the quantum defect between pump and signal wavelengths (2.6%), with other sources of loss such as background loss, back-scattered signal and ASE (forward and backward) being negligible.

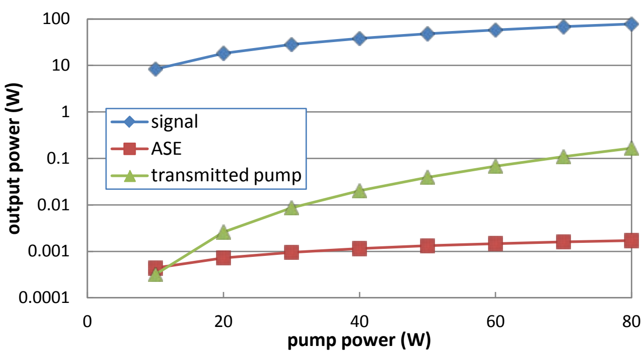

Fig. 4 Average Output signal and ASE powers as a function of average input pump power for 1.5 m fiber, shown on a log scale together with ASE and transmitted pump powers (repetition rate 10kHz).

Figure 4 shows output powers of the signal, unabsorbed pump and forward ASE on a log scale as a function of pump power. (At 10 kHz a power of 10 W corresponds to 1 mJ total pulse train energy). The ASE power remains at ~ -45 dB of signal power for all signal pulse energies. This is a ~20 dB reduction in ASE level compared with c.w. pumping. The ratio of unabsorbed pump to signal rises with output power but remains well below -20 dB for all pulse energies considered.

IV. Impact on Thresholds for Nonlinear Interactions

The simulations do not deal with nonlinearity, but a reasonable estimate for the practical limit on peak power of a signal travelling in the fiber which will not result in nonlinear distortion is the threshold for stimulated Raman scattering (SRS), which is approximated by:

$$P^{P}_{Critical} = 16 A_{eff} \mathrm{K} / (g_R L_{eff}) \qquad (1)$$

where g_R is the Raman gain coefficient for silica, L_{eff} is the effective length of the fiber (i.e. the length over which signal power is greater than P_{out}/e) and K=2 for unpolarised or circularly polarized light [24].

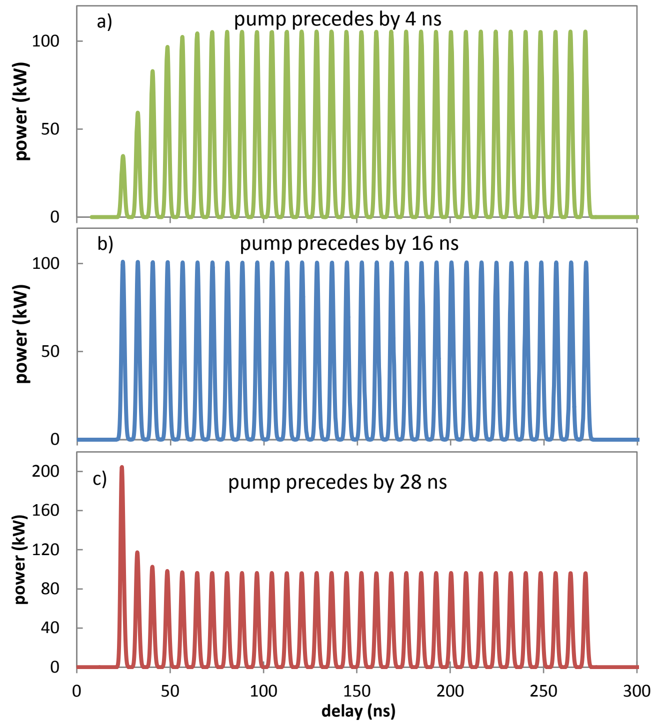

Fig. 5 Pulse train for overlapped pulsed pumping with various delays between the start of the pump and the peak of the first signal pulse of a) 4 ns and b) 16 ns and c) 28ns for 6.8 mJ power in output pulse train.

As can be seen in Fig. 2, in the initial section of the fiber, where the inversion is clamped at the maximum inversion for the pump wavelength, the signal experiences a constant, very high gain (~22 dB/m). If one were to operate purely in the unsaturated gain regime at a fiber length where there was significant unabsorbed pump, this would yield an L_{eff} for the amplifier of as low as 14 cm. In practice, to achieve reasonable conversion efficiency we need to extend the fiber beyond this region. If we select a length of 1.3 m, we still have an L_{eff} of just 40 cm (compared to 60cm for the 1.5 m length chosen for optimum ASE suppression). These values are not strongly dependent on pulse energy. For L_{eff}=40 cm, eqn.1 gives a value for the SRS threshold of 104 kW. If we assume that each pulse in the output pulse train has the same peak power, this gives us an estimate for the maximum total pulse energy before nonlinear interactions significantly distort the spectrum of the pulse, of 6.8 mJ in our 32 pulse train. The reduction in length from 1.5 m to 1.3 m leads to a slight reduction in efficiency (~3%) and small increase in unabsorbed pump (which could be removed using a dichroic filter).

Although this illustration shows that the optimum length depends on whether gain-dynamics or the mitigation of nonlinear effects is selected as the most important optimization criterion, in practice, the achievable pulse energy will also be strongly dependent on saturation effects in the amplifier, which can potentially strongly reshape the pulse train, meaning that individual pulses at the leading edge of the pulse burst may exceed the peak power limit for SRS even if the total energy in the pulse train is low.

Figure 5 shows pulse trains produced by overlapped pulsed pumping. To equalize all the pulses, the initial pulse should experience the same inversion as subsequent pulses, there needs to be an initial pumping period before the first pulse which is relatively long compared to the spacing of the pulses, so that the first pulse experiences the same inversion as subsequent pulses. To achieve the correct pre-signal pumping time, simulations were tested with a variety of pump pulse start times but where the pump always ends at the same time as the signal pulse train and where the amplitude was adjusted so that the total pump pulse energy remains constant. For a pulse train of total output energy 6.6 mJ, the delay between the start of the pump pulse and the start of the first signal pulse was varied. Fig 5 a), b) and c) show examples where the initial pumping period was too short, optimized and too long respectively. In the results shown in Fig. 5b) the simulation yielded a peak power of ~100 kW for each pulse, i.e. matched to the calculated SRS threshold. The optimum value of the delay between pump and signal will depend on the energy of the pump pulse, the fiber geometry and the absorption and emission cross-sections. Non-overlapped or c.w. pumping produces an extreme version of the effect of starting the pump pulse too early. Reshaping becomes so strong that, if the first pulse peak power is required to be kept below the 100 kW limit, the 32 pulse train can have a total energy of no more than 0.88 mJ.

A minor point is that the temporal profiles of the individual pulses do experience some weak gain-related reshaping which distorts slightly their initially Gaussian profile at the input. This occurs because they still have a significant energy compared to the saturation energy of the fiber. However, for this particular pulse shape the effect on peak power is quite small. It should also be noted that varying the start delay in this way has negligible effect on the dynamics shown in section III.

In a pre-shaped pulse burst, the significant change in gain and Yb-inversion experienced by the first and last pulses would result in the pulses having different accumulated phase delay due to the Kramers-Kronig effect relevant for the Yb ions embedded in the matrix of the fiber. Furthermore as the peak power vs. position in the fiber is considerably different comparing the first and last pulses, the B-integral would be different for individual pulses. Hence, the avoidance of pre-shaping has considerable attractions for pulse-stacking or cavity enhancement schemes [25] that require every pulse in the burst to have uniform phase so they can be coherently combined with high efficiency.

The overall result shows this approach both removes the pulse energy constraints imposed by the unfavourable gain dynamics inherent in other pumping schemes, and greatly improves the nonlinear characteristics of the amplifier, both by reducing the reshaping of the pulse train and by reducing the nonlinear interaction length. In the case considered here this increases the maximum extractable energy by a factor of ~8.

Finally we considered the degradation of performance that can be expected if the pump pulse extends beyond the end of the signal pulse. At the power level considered here, extending the square pump pulse beyond the end of the signal pulse by 8 ns doubles the ASE output and increases the transmitted pump by 10%. As the unutilized pump saturates the amplifier, the transmitted pump rises sharply and signal power drops. With increasing pump tail length, the ASE level continues to rise until for 30 ns and longer tails it reaches about 10 times the optimized level and the signal power drops by 4%.

In the simulations above we have assumed a top-hat pulse temporal profile. Any deviation from this in the rising edge of the pulse will have negligible effect on the shaping of the signal pulses, since it is the pulse energy provided before the first signal pulse which determines the initial inversion and thus the first pulse height. Any ripple in the section of the pulse which coincides with the signal pulses will be reproduced in the shape of the output signal pulse train since individual pulses will see varying inversion. A slow falling edge for the pump pulse will produce excess ASE in the same way that an overlong pump pulse does.

We note that a possible limiting factor which needs to be considered is the nonlinear evolution of the pump. The input pump pulse has lower peak power than the signal (by a factor of about 3.6 in our simulations), because the pump power is constant throughout its duration, whereas signal pulses have only ~20% duty cycle within their allotted time-slots. Furthermore, the pump pulses also have a considerably longer effective nonlinear interaction length. The pump experiences only low absorption in the first ~1 m of the fiber and then strong absorption thereafter, so the effective nonlinear length can be approximated as ~1 m. In our simulations the SRS threshold is reached at higher pulse energies for the pump than the signal, so it is the signal peak power that is limiting, but this might not be the case for other signal pulse shape parameters.

V. Possible Pumping Schemes

Some consideration should be given to the availability of a pump laser for this device. Ideally the pump should produce multi-mJ, single mode, flat-top pulses. More practically, we might consider a compromise approach, where a fairy high brightness weakly multi-mode source is launched into a raised index inner cladding slightly larger than the core of the signal fiber.

As an example, we consider a fiber similar to the amplifier fiber discussed above (see section II), but where the 14 μm diameter (NA 0.1) core is surrounded by a raised index inner cladding of 37 μm diameter (NA 0.16), with the core index raised so that the core/inner cladding index difference matches the core/clad index difference of the original fiber. The signal mode is negligibly affected by this change. The pump overlap with the core will depend on the modal content of the pump signal, but it is a reasonable approximation that it will scale by the core/inner cladding area ratio compared to the core pumped case. In this case, the required pump could be realized as a multi-mode fiber amplifier or by spatially combined single-mode amplifiers (through SM-to-MM combiners [26]). A fiber amplifier with a 100 μm core and NA 0.06 could be coupled with high efficiency into the inner cladding. Such an amplifier would have a saturation energy of ~3.4 mJ at 1018 nm and could deliver a square 7 mJ, 250 ns pulse with a reasonable level of pre-shaping of a seed pulse (less than 10 dB from front to back), easily achievable with an acousto-optic or electro-optic modulator [27, 28].

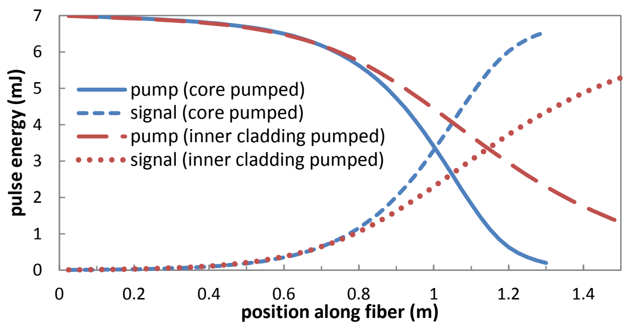

Fig. 6 Comparison of gain dynamics for core pumping (with 1.3m amplifier length) and pumping in a 37 µm diameter inner cladding (with 1.5m amplifier length), for pump pulses of 7 mJ.

Fig 6. compares this inner-clad pumping with the core pumped regime described above. Decreasing the pump overlap has the effect of increasing the length over which the unabsorbed pump is significant but the pump intensity is no longer sufficient to saturate the inversion in the fiber, and hence the growth of the signal is more gradual. (The effect on the ASE is very small.) It remains about 45 dB lower than the signal power for all the pulse energies and fiber lengths considered. The effect on the nonlinear length and on the fraction of transmitted pump is more significant and hence avoiding SRS requires a trade-off with efficiency. As shown in Fig. 6, setting the fiber length at 1.5 m results in 20% transmission of unabsorbed pump, and an L_{eff} for the signal of ~53 cm, giving a peak power limit of about 75 kW, and a corresponding pulse energy limit of 5.1 mJ. Increasing the fiber length to increase the pump absorption will push the achievable peak powers/ pulse energy down. Decreasing it from this value rapidly increases the lost pump. However, it should be noted that, because the reduced efficiency is due to unabsorbed pump at the output of the fiber, the benefits in thermal stability due to in-band pumping are not compromised. The attractions of c.w. tandem pumping for Yb fiber amplifiers have led to high power short-wavelength pump fiber lasers being developed [29-31]. The additional benefits of sub-µs duration, overlapped pulse pumping as outlined here may well encourage further experimental research.

VI. Discussion

The fundamental novelty of pulsed pumping has been enabled by considering the pump laser as a highly-engineered fiber laser that performs not only the functions of brightness enhancement and thermal management, encountered in c.w. tandem pumping, but also provides energy storage. Hence, a new regime of pumping can be considered with peak powers that are hundreds of times larger than the average power. This is possible because, unlike diode pumps, the fiber tandem pump lasers can store considerable amounts of energy between pulses.

We simulated results specifically for Yb-doped fibers as they currently set the benchmark for what is achievable with high average power fiber lasers. However, the technique is applicable to all fiber amplifiers based on rare-earth transitions sharing a common lower level for pump and signal e.g. Er, Tm and will also be useful for Tm pumped Ho fibers.

The long upper-state lifetime of the Yb ions enables a previously inaccessible regime of pulsed pumping in fiber lasers. This can be considered as an extension of the way a Q-switched pump laser is used to pump Ti:Sapphire CPA systems with regenerative or multipass final amplifiers operating at kHz repetition rates with ~5 W average power, but in the case of fibers the efficient thermal management provided by the geometry enables scaling to MHz or GHz repetition rates and much higher average powers. While there are clear questions that will need to be addressed in regard to the optimum combination of pump laser fiber and final amplifier fiber, it is likely that these issues will be tackled in the required level of detail only once experimental work in the field is underway.

The cost and complexity of a single fiber amplifier will increase compared to that of the conventional rod-type-amplifier with 975 nm diode used in a cladding pumped configuration due to the requirement for the intermediate pump (fiber) laser. Probable initial uses would be (a) to operate at power levels above the limit set by transverse mode instability in rod-fibers, because of the much reduced thermal load due to in-band pumping; (b) in large multi-channel facilities [32] where the added cost of the more-complex gain block in the amplifier is more than compensated by reduced maintenance and running costs as well as simplified control and environmental engineering enabled by the fiberized tandem pump laser and increased operating lifetime provided by an amplifier that is operated in a setup resistant to photodarkening related effects, because of the drastically reduced average inversion due to inband pumping and the low duty cycle of pulsed pumping.

Overlapped pulse pumping as reported here is a particularly advantageous example of tandem pumping which may have applications for very high power pulsed fiber lasers. In the case of c.w. pumping, or with pump pulses which do not overlap temporally with the signal pulse, there is a very definite limit to the pulse energy which can be extracted. In ref. 11, using the same fiber parameters used in this paper, we obtained a maximum attainable pulse energy of ~2 mJ. With a temporally overlapped pump pulse this limit, which is due to the finite energy storable in the fiber, is not observed since energy is being extracted by the signal pulse train at the same time it is being injected by the pump. When comparing the results in detail, it is notable that Fig. 2 showed that the ~1.5 m interaction distance over which pump absorption is achieved is not strongly dependent on pump/signal pulse energy, unlike tandem pumping with a c.w. or non-overlapped pulsed pump where the interaction length is roughly proportional to the pump pulse energy. Then Fig. 4. shows that with simulations for 7 mJ pulse energy produced a similar level of ASE and unabsorbed pump to those obtained for non-overlapped pulses at the optimum pump pulse energy for ASE suppression in that case of ~1.7 mJ. However, with non-overlapped pulses we found that both ASE and transmitted pump rise sharply if the system is pumped harder (results not shown for brevity), and the signal pulse energy is clamped. This hard limit is not encountered with overlapped pulses and the maximum energy is controlled first by the achievable peak power (SRS) and the burst duration and ultimately the extractable energy is also controlled by the achievable pump pulse energy from the tandem pump laser.

Also important is that in the case of c.w. or non-overlapping pulsed pumping, very strong reshaping of the pulse train is observed, as the inversion changes substantially between the passage of the first and last pulses in each burst. Figure 5 shows that careful timing of the onset of the pump pulse can eliminate this, producing a pulse train in which each pulse has equal energy.

A similar in-band pumping scheme using a pulsed pump launched into the core or a mini-pedestal of a signal amplifier might be realised using a 976 nm pulsed fiber laser as pump. Pumping at 976 nm would decrease the length of the device compared to in-band pumping, reducing nonlinear effects. However, the shift of the signal to ~1030 nm to match the shifted gain peak would mean that it experienced much stronger reshaping due to its reduced saturation energy, meaning that the energy of individual pulses in the pulse-train might have to be reduced. Also, the approximately doubled quantum defect combined with the shorter length would significantly increase the thermal load. Furthermore, realising sufficiently high energy pump pulses would be a fundamentally greater challenge at 976 nm, due to the much reduced saturation energy compared to 1018 nm [33, 34]. Hence the advantages of the scheme are balanced by the increased technical challenges.

VII. Conclusions

The proposed amplification scheme has the usual advantages of tandem pumping i.e. high efficiency and low heat load. Furthermore, pulsed tandem pumping significantly reduces ASE and nonlinear limitations compared to c.w. tandem pumping. Here we have shown that when the pump pulse is temporally overlapped with the signal pulse train, the total output energy is not limited by saturation of the inversion (as it is in non-overlapped pulsed or c.w. pumping), and the achievable pulse train energy can be increased until nonlinearity becomes the limiting performance factor.

Reshaping of the pulse train due to gain dynamics is reduced significantly compared to c.w. or non-overlapped pulsed pumping if the start delay between the pump pulse and the start of the signal pulse train is set appropriately. This enables flat topped output pulse trains to be produced at pulse energies far in excess of those which could be achieved by pre-shaping the pulses via optical gating in a conventional pumping scheme.

The rapid transfer of pump to signal also results in an effective nonlinear length that is also very low (~40 cm) for the final amplifier. The flattening of the pulse train and the low L_{eff} both contribute to allowing much higher energy in the pulse chain before the onset of nonlinear effects. For the pulse train described here, this increased the viable energy for the signal pulse train by a factor of 8 compared to c.w. pumping. The uniformity of the gain from the start to the end of the pulse-train removes phase differences that would otherwise arise from variable amounts of SPM from the silica nonlinearity or Kramers-Kronig phase from the change in inversion of the active Yb-ions.

The fiber we have simulated has relatively modest core size. For both the gain dynamics and nonlinear calculations, powers and pulse energies will scale simply with A_{eff} for any single-mode fiber, so larger-cored fibers will have proportionally increased limits on pulse energies and peak powers. Average powers can be further scaled (potentially up to kW levels) simply by increasing the number of pulses in each pulse burst or the repetition rate between pulse bursts. The challenge in developing this system is likely to be the availability of sufficiently bright pumps, which can also provide the required pulse energy at ~1018nm. However, the use of a final amplifier fiber with a small inner cladding to achieve close-area-ratio pumping offers the possibility to utilize most of the advantage described above, using achievable pump sources.

This new regime of overlapped tandem pulsed-pumping offers many benefits for the currently envisioned parallel and coherently combined multi-channel high energy, high average power, picosecond and femtosecond pulse fiber lasers being considered for future scientific, industrial and space-based applications.

We thank Prof. J. Nilsson and Prof. Sir D.N. Payne for their encouragement of this research and for useful discussions.

References

[1] M. N. Zervas and C. A. Codemard, "High Power Fiber Lasers: A Review," *Selected Topics in Quantum Electronics, IEEE Journal of,* vol. 20, pp. 219-241, Sep-Oct 2014.

[2] J. Zhu, P. Zhou, Y. Ma, X. Xu, and Z. Liu, "Power scaling analysis of tandem-pumped Yb-doped fiber lasers and amplifiers," *Optics Express,* vol. 19, pp. 18645-18654, 12 Sept. 2011.

[3] Y. Zhu, P. Zhou, H. Zhang, X. Wang, and S. Guo, "Analysis of the power scaling of resonantly pumped Tm-doped silica fiber lasers," in *International Symposium on Photoelectronic Detection and Imaging: High Power Lasers and Applications*, , 2013, pp. 89040R-89040R-8.

[4] Y. M. Chang, T. Yao, H. Jeong, J. Ji, S. Yoo, T. C. May-Smith, *et al.*, "3 % Thermal Load Measured in Tandem-pumped Ytterbium-doped Fiber Amplifier," in *CLEO:* San Jose, California, 2014, p. STh4N.7.

[5] A. Ferin, V. Gapontsev, V. Fomin, A. Abramov, M. Abramov, and D. Mochalov, "17 kW CW laser with 50 µm delivery," in *6th International Symposium on High-Power Fiber Lasers and Their Applications*, St Petersburg, 2012.

[6] E. Shcherbakov, V. Fomin, A. Abramov, A. Ferin, D. Mochalov, and V. P. Gapontsev, "Industrial Grade 100 kW Power CW Fiber Laser," in *Advanced Solid-State Lasers Congress*, Paris, France, 2013, p. ATh4A.2.

[7] G. Mourou, B. Brocklesby, T. Tajima, and J. Limpert, "The future is fibre accelerators," *Nat Photon,* vol. 7, pp. 258-261, 2013.

[8] R. Soulard, M. N. Quinn, T. Tajima, and G. Mourou, "ICAN: A novel laser architecture for space debris removal," *Acta Astronautica,* vol. 105, pp. 192-200, December 2014.

[9] C. Jauregui, H.-J. Otto, N. Modsching, J. Limpert, and A. Tünnermann, "Recent progress in the understanding of mode instabilities," in *Photonics West: , Fiber Lasers XII: Technology, Systems, and Applications*, San Francisco, 2015, pp. 93440J-1-6.

[10] M. N. Zervas, "TMI Threshold in High Power Fiber Amplifiers," in *Advanced Photonics 2016 (IPR, NOMA, Sensors, Networks, SPPCom, SOF)*, Vancouver, Canada, 2016, p. SoW2H.2.

[11] A. Malinowski, J. H. V. Price, and M. N. Zervas, "Sub-Microsecond Pulsed Pumping as a Means of Suppressing Amplified Spontaneous Emission in Tandem Pumped Fiber Amplifiers," *IEEE Journal of Quantum Electronics*, vol. 51, pp. 6800307-1-7, 2015.

[12] M. Lapczyna, K. P. Chen, P. R. Herman, H. W. Tan, and R. S. Marjoribanks, "Ultra high repetition rate (133 MHz) laser ablation of aluminum with 1.2-ps pulses," *Applied Physics A*, vol. 69, pp. S883-S886, 01 December 1999.

[13] I. Will, H. I. Templin, S. Schreiber, and W. Sandner, "Photoinjector drive laser of the FLASH FEL," *Optics Express*, vol. 19, pp. 23770-23781, 21 Nov. 2011.

[14] P. Elahi, S. Yılmaz, Y. B. Eldeniz, and F. Ö. Ilday, "Generation of picosecond pulses directly from a 100W, burst-mode, doping-managed Yb-doped fiber amplifier," *Optics Letters*, vol. 39, pp. 236-239, 15 Jan. 2014.

[15] C. Kerse, H. Kalaycıoğlu, P. Elahi, B. Çetin, D. K. Kesim, Ö. Akçaalan*, et al.*, "Ablation-cooled material removal with ultrafast bursts of pulses," *Nature*, 07/13/online 2016.

[16] S. Zhou, F. W. Wise, and D. G. Ouzounov, "Divided-pulse amplification of ultrashort pulses," *Optics Letters*, vol. 32, pp. 871-873, 1 April 2007.

[17] M. Kienel, A. Klenke, T. Eidam, S. Hädrich, J. Limpert, and A. Tünnermann, "Energy scaling of femtosecond amplifiers using actively controlled divided-pulse amplification," *Optics Letters*, vol. 39, pp. 1049-1052, 2014/02/15 2014.

[18] K. W. Morton and D. F. Mayers, *Numerical solution of partial differential equations: an introduction*, 2nd ed.: Cambridge University Press, 2005.

[19] C. R. Giles and E. Desurvire, "Modeling Erbium-Doped Fiber Amplifiers," *Journal of Lightwave Technology*, vol. 9, pp. 271-283, Feb 1991.

[20] R. Paschotta, J. Nilsson, A. C. Tropper, and D. C. Hanna, "Ytterbium-doped fiber amplifiers," *IEEE Journal of Quantum Electronics*, vol. 33, pp. 1049-1056, Jul 1997.

[21] H. M. Pask, R. J. Carman, D. C. Hanna, A. C. Tropper, C. J. Mackechnie, P. R. Barber*, et al.*, "Ytterbium-Doped Silica Fiber Lasers - Versatile Sources for the 1-1.2 micron Region," *IEEE Journal of Selected Topics in Quantum Electronics*, vol. 1, pp. 2-13, Apr 1995.

[22] A. H. Hartog and M. P. Gold, "On the theory of backscattering in single-mode optical fibers," *Journal of Lightwave Technology*, vol. 2, pp. 76-82, 1984.

[23] M. N. Zervas and R. Laming, "Rayleigh scattering effect on the gain efficiency and noise of erbium-doped fiber amplifiers," *Quantum Electronics, IEEE Journal of*, vol. 31, pp. 468-471, 1995.

[24] R. G. Smith, "Optical power handling capacity of low loss optical fibers as determined by stimulated Raman and Brillouin scattering," *Applied Optics*, vol. 11, pp. 2489 - 2494, 1972.

[25] H. Carstens, M. Högner, T. Saule, S. Holzberger, N. Lilienfein, A. Guggenmos*, et al.*, "Cavity-enhanced high-harmonic generation at 250 MHz," in *High-Brightness Sources and Light-Driven Interactions*, Long Beach, California, 2016, p. HM6B.6.

[26] S. Hong-Seok, A. Joon Tae, P. Bong Je, S. Jung-Ho, and C. Woonjin, "Efficient Pump Beam Multiplexer Based on Single-Mode Fibers," *Japanese Journal of Applied Physics*, vol. 51, p. 010203, 2012.

[27] D. N. Schimpf, C. Ruchert, D. Nodop, J. Limpert, A. Tünnermann, and F. Salin, "Compensation of pulse-distortion in saturated laser amplifiers," *Optics Express*, vol. 16, pp. 17637-17646, 2008.

[28] A. Malinowski, K. T. Vu, K. K. Chen, J. Nilsson, Y. Jeong, S. Alam*, et al.*, "High power pulsed fiber MOPA system incorporating electro-optic modulator based adaptive pulse shaping," *Optics Express*, vol. 17, pp. 20927-20937, 9 Nov. 2009.

[29] F. Beier, H. J. Otto, C. Jauregui, O. de Vries, T. Schreiber, J. Limpert*, et al.*, "1009 nm continuous-wave Ytterbium-doped fiber amplifier emitting 146 W," *Optics Letters*, vol. 39, pp. 3725-3727, 01 July 2014.

[30] G. Gu, Z. Liu, F. Kong, H. Tam, R. K. Shori, and L. Dong, "Highly efficient ytterbium-doped phosphosilicate fiber lasers operating below 1020nm," *Optics Express*, vol. 23, pp. 17693-17700, 13 July 2015.

[31] H. Xiao, P. Zhou, X. L. Wang, X. J. Xu, and Z. J. Liu, "High power 1018 nm ytterbium doped fiber laser with an output power of 309 W," *Laser Physics Letters*, vol. 10, p. 065102, 2013.

[32] W. S. Brocklesby, J. Nilsson, T. Schreiber, J. Limpert, A. Brignon, J. Bourderionnet*, et al.*, "ICAN as a new laser paradigm for high energy, high average power femtosecond pulses," *The European Physical Journal Special Topics*, vol. 223, pp. 1189-1195, y 2014.

[33] J. He, S. Du, Z. Wang, Z. Wang, J. Zhou, and Q. Lou, "Linearly-polarized short-pulse AOM Q-switched 978 nm photonic crystal fiber laser," *Optics Express*, vol. 21, pp. 29249-29254, 2013.

[34] R. Selvas, J. K. Sahu, J. Nilsson, S. A. Alam, and A. B. Grudinin, "Q-switched 980 nm Yb-doped fiber laser," in *Lasers and Electro-Optics. CLEO, Technical Digest, CThR6*, 2002, pp. 565-566 Vol.1.

Dr. Andrew Malinowski received a BA in Natural Sciences from the University of Cambridge in 1992 and a PhD in Physics from the University of Southampton in 1996.

He has worked at the University of Sheffield (1996-97) and the University of Southampton (1997-2011). Since 2011 he has been with SPI Lasers, Southampton, UK, working on fiber laser development.

Dr. Jonathan H. V. Price received the Ph.D. degree in optoelectronics from the Optoelectronics Research Centre, University of Southampton, U.K., in 2003.

He then held a Royal Academy of Engineering Postdoctoral Research Fellowship at the Optoelectronics Research Centre, University of Southampton and has continued working in his main research areas of applied nonlinear fiber optics using novel glass types as well as silica microstructured optical fibers for ultrashort-pulse wavelength conversion applications / supercontinuum generation and the development of high-power femtosecond pulsed fiber laser sources.

Prof. Michalis N. Zervas graduated from the Electrical Engineering Department, University of Thessaloniki, Thessaloniki, Greece, in 1984. He received the M.Sc. degree in applied and modern optics (with distinction) from the University of Reading, U.K., in 1985 and the Ph.D. degree in fiber optics from University College London, UK. in 1989.

He joined the Optoelectronics Research Centre, University of Southampton, Southampton, U.K., in 1991. In 2016 he was awarded a Royal Academy of Engineering Research Chair. His research activities include advanced optical fiber amplifier configurations, high-power fiber lasers and applications, fiber distributed feedback (DFB) lasers, Bragg grating theory and devices, surface-plasmon effects and devices, optical microresonators, and nonlinear fiber optics. He is a cofounder of Southampton Photonics Inc., where he is currently serving as Chief Scientist.

He has authored/coauthored over 300 technical publications, about 40 patents/patent applications, of which 20 are granted, and has served on various conference program committees. In 1996, he shared the prestigious Metrology award from the Confederation of British Industry for his work on grating measuring systems for characterizing reflection and dispersion performance of fiber Bragg gratings. He was elected OSA Fellow in 2015.